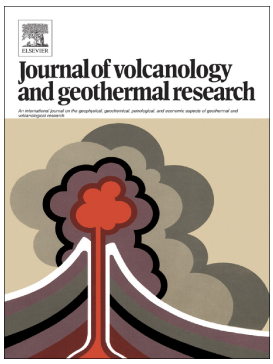

Widespread volcanism Southeast of Futuna Island (SW Pacific Ocean): Near-seafloor magnetic dating and regional consequences

Florent Szitkar, Jérôme Dyment, Yves Fouquet

PII: S0377-0273(20)30350-4

DOI: https://doi.org/10.1016/j.jvolgeores.2020.107064

Reference: VOLGEO 107064

To appear in: *Journal of Volcanology and Geothermal Research*

Received date: 24 June 2020

Revised date: 12 September 2020

Accepted date: 13 September 2020

Please cite this article as: F. Szitkar, J. Dyment and Y. Fouquet, Widespread volcanism Southeast of Futuna Island (SW Pacific Ocean): Near-seafloor magnetic dating and regional consequences, *Journal of Volcanology and Geothermal Research* (2020), https://doi.org/10.1016/j.jvolgeores.2020.107064

Widespread volcanism Southeast of Futuna Island (SW Pacific Ocean): Near-seafloor magnetic dating and regional consequences

Florent Szitkar[(1)], Jérôme Dyment[(2)], Yves Fouquet[(3)]

[(1)] NGU, The Geological Survey of Norway, Trondheim, Norway

[(2)] Institut de Physique du Globe de Paris, CNRS, Paris, France

[(3)] Ifremer, GM, F-29280 Plouzané, France

ABSTRACT

Near-seafloor bathymetric and magnetic data have been collected by Autonomous Underwater Vehicle (AUV) and manned submersible (DSS) over a volcanically active area southeast of Futuna Island, French Territory of Wallis-and-Futuna, in the Southwestern Pacific Ocean. Located at the edge of the Lau and North Fiji basins, at the convergence of the Pacific and Australian plates, this area is characterized by intense volcanic and tectonic activity. Direct observation by submersible reveals that the seafloor is covered by recent lava flows, volcanoes and large, active or inactive calderas filled by smooth lava flows and eventually hosting hydrothermal sites. We investigate the volcanic chronology by combining a Bayesian inversion of the AUV-gridded magnetic data with an inversion of the submersible data specifically designed to estimate the rock magnetic polarity and absolute magnetization. We show that some volcanoes predate the last (Brunhes-Matuyama) magnetic polarity reversal 780 kyr ago whereas their neighbors exhibit a normal polarity and

appear to be recent. This result suggests that the seafloor in this region has undergone continuous and sparse volcanic activity over the last few million years.

1) Introduction

The most active volcanic area in the world, known as the Pacific Ring of Fire, encompasses the Pacific Ocean and marks the limits of the Pacific Plate. To the South-West, this plate subducts beneath the Australian plate and forms the Tonga Trench. West of the trench, the Kermadec volcanic arc and the Lau back-arc basin are made of the several inferred small plates (e.g., Bird, 2003). Near its northern end, the Tonga Trench winds Westwards and connects to a complex system of strike-slip faults and volcanic ridge segments within the Northern Lau Basin (Pelletier et al., 2001; Wright et al., 2000). Southeast of Futuna Island lies a volcanically complex area characterized by relatively shallow depths and intense volcanic and hydrothermal activity (e.g., Fouquet et al., 1991; Fouquet et al., 1993; Baker et al., 2005, Labanieh et al., 2011; Lupton et al., 2015, Sleeper and Martinez, 2016). This area does not present the morphology of a spreading center but defines a roughly 100x100 km^2 (Fig. 1) diffuse volcanic province instead (Pelletier et al., 2001). We use a combination of regional and high-resolution bathymetric and magnetic data respectively collected at the sea surface by R/V *L'Atalante* and near seafloor by Autonomous Underwater Vehicle (AUV) *Idef-X* or Deep-Sea manned Submersible (DSS) *Nautile* to investigate some major volcanic edifices and unravel the chronology of their emplacement. Combining a Bayesian inversion of the AUV-gridded magnetic data (Honsho et al., 2012) with an inversion of the submersible data specifically designed to estimate the rock magnetic polarity and absolute magnetization (Szitkar et al., 2015a), we show that the volcanic activity started before the last magnetic

polarity reversal (780 ka) and has been continuous ever since, with no signs of waning. Such "intraplate" (i.e. off the well-defined plate boundaries) volcanic activity may result from melting of the underlying Indian ocean-type mantle and an additional input driven by the Samoa hotspot (Jackson et al., 2010; Jenner et al., 2012). Such intense volcanic activity likely plays an important role in remodeling the small plates constituting the Northern Lau Basin.

2) Geological context

Futuna island is part of the French overseas territory of Wallis-and-Futuna, in the South Pacific, roughly halfway between Samoa and Fiji. Wallis and Futuna islands are separated by a fossil subduction zone, the Vitiaz Trench, where water depths largely exceed 4500 m, in the direct continuation of the Tonga Trench (Brocher et al., 1985). This fossil subduction is a key element to the geological evolution of the Southwestern Pacific, as it delineates the border between the Cretaceous Pacific Plate to the North and the Cenozoic North-Fiji and Lau Basins to the South (e.g., Pelletier et al., 1998).

Previous research carried out on Futuna island has revealed the existence of volcanic structures dated Upper Pliocene and made of pillow lavas, breccias, hyaloclastites and massive lava flows (Grzesczyk et al., 1987, 1988, 1991a, b). A switch in the volcanic activity at the end of the Pliocene is seen as a marker of a tectonic change from a subducting (Vitiaz-Tonga subduction) to a transform regime (North-Fiji transform fault).

In March 2000, cruise ALAUFI (Pelletier et al., 2001) discovered the Futuna Ridge, a spreading center extending over a distance of more than 200 km from the North of the Fiji platform to the Northwest of Futuna Island. It also revealed a 30 km-wide area with a WSW-ENE orientation between 176°30’ and 177°25’W centered at 14°45’S associated with a

shallower bathymetry and many volcanoes (Fig. 1). This region, now known as the South-East Futuna Volcanic Zone (SEFVZ), is defined by bathymetric lineations with a 80 - 90° orientation in its northern part and 50° in the Southwest, and is associated with a strong volcanic activity (Pelletier et al., 2001). Although the SEFVZ may be interpreted as another active spreading center in the northern Lau Basin, the lack of a clear topographic expression may also suggest diffuse magmatic activity over a wide area (Pelletier et al., 2001). While the Futuna Ridge exhibits a series of magnetic chrons 2 to 1 (Pelletier et al., 2001), the SEFVZ lacks any recognizable seafloor spreading anomalies and its age remains unconstrained. As shown below, deep-sea magnetic anomaly data provide some clue on this aspect.

3) Acquisition and Processing

Two scientific cruises, FUTUNA 2010 and 2012, were carried out by R/V *L'Atalante,* AUV *Aster*^{X} (in 2010) and *Idef*^{X} (in 2012) and DSS *Nautile.* They collected shipboard and high-resolution (AUV) bathymetry as well as shipboard and high-resolution (AUV and DSS) magnetic data. Three-component magnetometers were installed on both submersibles. Bathymetric mapping (Fig. 1) unveiled the existence of large calderas, including Kulo Lasi and Ono (Fig. 2 and 3), and wide volcanic areas, such as Fatu Kapa (Fouquet et al. 2018) and Tasi Tulo (Fig. 4A) (e.g., Konn et al., 2016; Konn et al., 2018).

The initial processing of the raw magnetic data is comparable to that described in several other papers (Isezaki, 1986; Honsho et al., 2009; Szitkar et al., 2015b; Szitkar et al., 2017) (Supplementary Material). AUV dives were designed to survey large areas along regularly-spaced, 100 m-apart parallel profiles, and the data underwent a quick daily processing to identify geological features for DSS *Nautile* to dive on. Conversely, DSS *Nautile* explores the seafloor and carries out direct observation, geological mapping and collect rock, fluids and

biological samples. Its path is therefore not suitable for gridding the magnetic data. Due to the proximity of the seafloor, these data also show shorter-wavelengths and higher amplitudes than those collected by AUV dives at higher altitudes above the seafloor (on average 70 m above the seafloor). Since the depth of sources depicted by magnetic anomalies directly depends on the altitude of the measurements, DSS *Nautile* data mostly depict outcropping small sources whereas AUV data reflect slightly deeper sources.

We take advantage of the peculiarities of DSS *Nautile* dives, including its strongly varying altitude above the seafloor, to estimate the absolute magnetization and magnetic polarity of the shallow subsurface magnetic sources (Honsho et al., 2009; Szitkar et al., 2015a Constraining magnetic polarity represents a key parameter for constraining the age of volcanic edifices beyond the freshness of the topographic expression, backscatter intensity, and direct evidence.

For the AUV data, we applied the Honsho et al. (2012) Bayesian inversion that considers the varying AUV altitude above the seafloor and preserves the full-wavelength content of the signal to compute an equivalent magnetization and a rigorous Reduced-to-the-Pole (RTP) anomaly (i.e. in the geometry of the experiment and assuming a vertical geomagnetic field; Supplementary Material) (Fig. 2, 3, 4, 5).

4) Results

4.1) Kulo Lasi Caldera

The first major target to be investigated during cruise Futuna 2010 was the Kulo Lasi Caldera (Fouquet et al., 2018; Fig. 2). This roughly circular caldera, ~5 km in diameter, is flanked by two small volcanoes to the Northeast and to the West. The caldera floor lies at ~1500 m bsl

and exhibits a smooth bathymetry, apart from a central, faulted resurgent dome (Fig. 2A). A total of six AUV dives surveyed the whole caldera and six DSS *Nautile* dives investigated specific targets. The equivalent magnetization (Fig. 2B) and RTP magnetic anomaly (Fig. 2C) reveal highly magnetized areas, mostly on top of the two nearby volcanoes and at the top of the caldera walls. The magnetization is generally weaker on the caldera floor and the Northeastern part presents a lower RTP magnetic anomaly. The amplitude of RTP magnetic anomaly spans 50 000 nT.

On the caldera floor, DSS *Nautile* discovered abundant high and low-temperature hydrothermal activity with numerous small active and inactive sites. High $CH_4/^3He$ and CH_4/TDM ratios were reported in the hydrothermal plumes, these values being characteristic of an intense volcanic event in 2010 (Konn et al., 2016) followed by the widespread occurrence of extremely young high-temperature hydrothermal chimneys at the time of the dives, a few month later (Fouquet et al. 2018, Konn et al 2018). The sites are always associated with a negative RTP magnetic anomaly on the AUV map (Fig. 2B, 2C), in accordance with previous studies conducted over basalt-hosted or andesite-hosted hydrothermal systems in other (e.g., Tivey et al., 1993, Szitkar et al., 2014, Szitkar et al., 2015b, Fujii et al., 2015) and similar (Caratori Tontini et al., 2012; Honsho et al., 2013) geological contexts.

The absolute magnetization derived from DSS *Nautile* data (Supplementary Material) exhibits a strong intensity ranging between ~15 and 50 A/m. The distribution of magnetization is generally consistent at local scale, with patches of strong (~40-50 A/m) magnetization on smooth recent lava flows and weaker (~15-30 A/m) magnetization on faulted areas, particularly near the caldera walls. The corresponding polarities are dominantly normal, with a few reversed polarity areas near the caldera walls.

4.2) Ono Caldera

The Ono Caldera is located roughly 30 km WSW from the Kulo Lasi Caldera (Fig. 3). The high-resolution bathymetry reveals a uniformly smooth topography (Fig. 3A), suggesting that it has been covered by a significant accumulation of sediments. A group of N30°E faults appears on the bathymetric highs and cuts across the whole structure (Fig. 3A). Neither the AUV nor DSS *Nautile* have identified any evidence of recent volcanism or active hydrothermalism in this caldera. Unlike the Kulo Lasi Caldera, the Ono Caldera exhibits positive RTP magnetic anomaly (Fig. 3B) and equivalent magnetization (Fig. 3C) on its floor and negative anomalies on its crests where DSS *Nautile* observed the presence of outcropping basalt. The amplitude of the RTP magnetic anomaly spans 2000 nT.

The only DSS *Nautile* dive devoted to this caldera roughly followed the crests (Fig. 3D). The absolute magnetization is significantly weaker on Ono (0-12 A/m) than on Kulo Lasi and its polarity is systematically reversed.

4.3) Isolated volcanoes on Fatu Kapa area

The Fatu Kapa area is located 30 km North of the Kulo Lasi Caldera and has been surveyed by 15 AUV dives. The high-resolution bathymetry at the center of the Fatu Kapa area, (Fig. 4A) reveals a wide and relatively flat volcanic dome, 6-km in diameter, cut across by a series of roughly East-West normal faults and grabens. Successive tectonic and volcanic episodes result in a network of intersecting faults which favor the circulation of hydrothermal fluids (Fig. 4A). The magnetic data from AUV and DSS *Nautile* result in weak RTP anomalies, equivalent magnetization (AUV data) and absolute magnetization (DSS *Nautile* data) over

the newly discovered hydrothermal fields, as expected for basalt-hosted hydrothermal sites (Szitkar et al., 2015; Fouquet et al., 2015; Konn et al., 2018). The area is characterized by a strong backscatter (Fouquet at al., 2018, their Figure 3), and therefore fresh and young lava.

At the west and East of the main volcanic areas (Fig 3) several isolated volcanic edifices have been observed on the graben floor, two to the Southwest and a third one to the East (Fig. 4). Only AUV data are available there, as no DSS *Nautile* dive has been carried out on these volcanoes. On the high-resolution bathymetry, the two Southwestern volcanoes show no evidence of faulting whereas the Eastern volcano has E-W tissures and small-offset normal faults (Fig. 4A). The three edifices display positive RTP magnetic anomalies and equivalent magnetization (Fig. 4B, 4C).

4.4) Tasi Tulo area

The Tasi Tulo area extends Northeast of the Fatu Kapa area (Fig. 5). It exhibits a number of volcanoes and has been surveyed by two AUV and two DSS *Nautile* dives. This area is characterized by a superposition of two types of volcanoes: six large, flat isolated edifices on one hand, and series of small conical mounds forming two volcanic ridges trending N60°E and N70°E on the other hand, both roughly aligning with the graben located further Northeast (Fig. 1). The flat volcanoes are faulted and partially overlapped by the ridges which do not exhibit major faults. The magnetic signature of the flat volcanoes varies: the smaller volcano A displays a simple positive equivalent magnetization and RTP magnetic anomaly (Fig. 5), as observed on the three studied volcanoes of the Fatu Kapa area. The larger volcanoes can be divided in two categories. Volcanoes B and E are characterized by a rim of strong positive equivalent magnetization surrounding an area of weak magnetization (Fig. 5) and are comparable to the Kulo Lasi caldera and its flanking volcanoes. Volcanoes D

and F display a rim of strong negative equivalent magnetization encompassing an area of weak equivalent magnetization, similar to Ono (Fig. 5). The magnetic signature of volcano C is unclear, and is probably hidden by the strong positive signature of the nearby volcanic ridge. Finally, the two ridges display a strong positive equivalent magnetization and RTP anomaly in the shallowest part of the survey (Fig. 5).

Direct observations from DSS *Nautile* as well as rock sample analyses indicate that the seafloor is made of recent basalt with little sediment cover. Magnetic data were only acquired during one of the two DSS *Nautile* dives and was mostly inconclusive. Our analysis therefore relies on the AUV data (Fig. 5).

5) Discussion

5.1) Kulo Lasi Caldera

The Kulo Lasi Caldera presents all the evidence of an active volcano. The smooth caldera floor is a direct consequence of its resurfacing by successive lava flows. Moreover, the AUV and DSS *Nautile* discovered several small active basalt-hosted hydrothermal systems. These sites are all associated with a lack of magnetization and even the smaller ones are depicted on the equivalent magnetization and RTP magnetic anomaly. An alignment of hydrothermal sites has been observed to the Northeast of the caldera, resulting in the elongated negative magnetic anomaly visible in this area (Fig. 2B, 2C). The limited size of these sites also supports the hypothesis of frequent resurfacing as sites do not have time to reach larger dimensions before being destroyed by and buried under new lava flows. The strong absolute magnetization derived from DSS *Nautile* data on the caldera floor confirms the very young age of the outcropping basalt, in agreement with the corresponding normal polarities. The areas of reverse polarities observed at the foot of the caldera walls likely correspond to

coherent tilted blocks that may have fallen from the walls. The magnetic signature of the Kulo Lasi caldera is therefore made of: (1) high magnetization on the crest of the caldera and the rim of the two flanking volcanoes; (2) a weaker magnetization on the floor; (3) local magnetic lows created by active and inactive hydrothermal sites; and (4) dominantly normal polarities with a few anomalous zones probably related to fallen blocks. Such a signature may be representative of a recent / active caldera formed during the Brunhes normal period.

5.2) Ono Caldera

The uniform sediment accumulation, the faults cross-cutting the whole caldera, the lack of recent volcanism and active hydrothermalism (Fig. 3a) suggest that the Ono Caldera is significantly older than the Kulo Lasi Caldera.

The RTP magnetic anomaly amplitude at Kulo Lasi reaches roughly 50.000 nT whereas that at Ono barely reaches 2000 nT, suggesting that the basalt magnetization at Ono is weaker than at Kulo Lasi. This observation could be explained by the progressive alteration of older rocks by seawater and would therefore support older rocks at Ono with respect to the fresh basalt at Kulo Lasi. For both calderas, the AUV was navigated at an average altitude of 70 m above the seafloor, suggesting that the comparison is meaningful. Deep-sea sediments are weakly magnetized and their contribution to the observed magnetic anomalies is negligible (e.g., Szitkar et al., 2015b). However, the unknown thickness of sediments at Ono is not considered in the inversion to equivalent magnetization. The real top of the magnetized layer is likely significantly deeper than the bathymetry, especially on the caldera floor. In terms of the RTP magnetic anomaly, this corresponds to an upward continuation which attenuates the anomaly amplitude and more specifically its short-wavelength content.

Comparing the RTP magnetic anomaly amplitude is therefore hazardous as long as the sediment thickness is unknown. Conversely, the shape of the RTP magnetic anomaly and equivalent magnetization distribution is of particular interest: they both are positive on the floor and negative on the crests of the Ono Caldera, systematically opposite to those observed on the Kulo Lasi Caldera. Moreover, the magnetization polarity deduced from DSS *Nautile* data (Fig. 3D) is uniformly reversed. These observations concur in demonstrating that the Ono Caldera was formed during a reversed polarity interval, most likely the Matuyama Period (2.59-0.78 Ma).

5.3) Fatu Kapa area

The strong backscatter of the Fatu Kapa area, similar and in continuity to that observed around the Kulo Lasi Caldera on the shipboard data (Fouquet et al., 2018; their Fig. 3), indicates that both areas are recent and probably of the same age. The faulted Eastern volcano inside the central graben is probably slightly older than the Southwestern pristine unfaulted volcanoes. The positive RTP magnetic anomaly and equivalent magnetization confirm that the three volcanoes likely postdate the Brunhes-Matuyama magnetic polarity reversal.

5.4) Tasi Tulo area

The equivalent magnetization and RTP magnetic anomaly display strong variations among the different volcanic structures of the area. The small flat volcano A associated with a positive RTP anomaly resembling that of the three Fatu Kapa volcanoes were clearly formed during a period of normal polarity, most likely the Brunhes period (0-0.78 Ma). Such is also the case of the large flat volcanoes B and E displaying a positive magnetic ring similar to

those of the Kulo Lasi Caldera and volcanoes. We cannot rule out the hypothesis that these volcanoes could be older than the Brunhes period, for instance from the Olduvai episode within the Matuyama period; however, the unfaulted aspect of these volcanoes makes this possibility very unlikely. Conversely, the large flat volcanoes D and F displaying a negative magnetic ring similar to that of the Ono Caldera were formed during a period of reverse polarity, most likely the Matuyama period (2.59-0.78 Ma). The two volcanic ridges topping the flat volcanoes exhibit a strong positive equivalent magnetization and RTP magnetic anomalies and are obviously recent, formed during the Brunhes normal polarity period. The Tasi Tulo area is therefore made of a succession and a superposition of volcanoes that are older and younger than the last magnetic polarity reversal, suggesting a continuous volcanic activity over at least the last million years, and possibly up to 2.5 million years.

5.5) Regional consequences

The magnetic analysis of volcanic edifices in four areas of the SEFVZ suggests the presence of recent and active volcanoes at Kulo Lasi, Fatu Kapa, and Tasi Tulo areas, whereas older inactive volcanoes are observed at Ono and Tasi Tulo areas. The structural expression of the active areas does not support the presence of a continuous spreading center but instead of isolated magmatic centers which tectonic connection is complex and mostly hidden by the recent lava flows (Fig. 1). The observation of two generations of volcanoes at Tasi Tulo supports episodic and unfocused magmatic events over a relatively wide (~100 km) area.

The northern North Fiji and Lau basins exhibit a variety of small plates whose definition and delimitation are still to be completed. A discontinuous belt of major volcanic edifices exists within 250 km from the fossil Vitiaz Trench, where the Pacific Plate was subducting below the Australian plate (see Ruellan and Lagabrielle, 2005, their Fig. 2) (Fig. 6). These edifices

are observed between 169 and 173°E north of the Hazel-Holmes and South Pandora spreading centers (Lagabrielle et al., 1996); between 173 and 178°E at the axis and north of the South Pandora and Tripartite spreading centers (Lagabrielle et al., 1996); between 179°E and 178°W north of the Futuna and North Cikopia spreading centers (Pelletier et al., 2001); between 179 and 177°W in our study area; between 177 and 175°W at the axis and north of the North-West Lau and Niuafo'ou spreading centers (the latter also known as Rochambeau Rifts; Lupton et al., 2012); and between 175 and 174°W on the Mangatolu Triple Junction and North-East Lau Spreading Center (e.g., Lupton et al., 2012). Although the location of these edifices suggests the slow melting of the remnant Pacific slab and magma ascent within the North Fiji and Lau basins, their geochemistry is more consistent with the melting of the underlying Indian ocean-type mantle and an additional input driven by the Samoa hotspot (Jackson et al., 2010; Jenner et al., 2012). The absence of a Nb anomaly characteristic of recycled lithospheric material in subduction zones and the major and trace element contents closer to those observed in Oceanic Island Basalts (OIB) indeed favors the presence of OIB material, either from the Samoa chain (Guivel et al., 1997) or the Cook-Austral chain (Price et al., 2016).

The occurrence of episodic magmatic events likely affects the distribution and stability of the plate boundaries and diffuse volcanic zones, with new potential boundaries initiating on the most prominent zones of weakness. This in turn explains the presence of many small plates in the northern Lau Basin and offers a mechanism to maintain the tectonic complexity of this area. The northern North Fiji and Lau basins are clearly complex and unstable in terms of plate tectonics, and may represent an analog of Archean seafloor dynamics with a hotter mantle, as suggested by Lagabrielle et al. (1997).

6) Conclusion

The northern North Fiji and Lau basins are made of a mosaic of small plates that remain difficult to precisely delineate and that lie on top of the fossil Vitiaz subduction zone. Regional, ship-based bathymetric data collected during campaigns FUTUNA 1 and 3 contribute to refine this model and allow precising the plate contours, particularly in the vicinity of Futuna Island with the definition of new micro-plates. Melting of the remnant slab results in an episodic magmatism that likely control the many spreading centers and zones of widespread volcanism in this area. Such a widespread volcanism and the associated hydrothermalism are observed in our study area, SE of Futuna Island, where no clearly defined spreading center has developed yet. Using high-resolution, near-seafloor geophysical data, we show that the volcanism has been active for the last 1 to 2.5 Ma, as demonstrated by the analysis of the magnetic signature of selected volcanic edifices in four detailed survey areas and the resulting magnetization polarity that encompasses the last magnetic polarity reversal, 0.780 Myr ago. High resolution magnetics better constrain the age of individual edifices in complex volcanic areas and provides further insight into the evolution of such areas..

Acknowledgements

We thank the captain and crew of R/V L'Atalante, the technical teams of AUV *Aster*^{X} and *Idef*^{X} and DSS *Nautile*, and the IFREMER scientific team for excellent work at sea during Cruises FUTUNA 2010 and 2012. IPGP, CNRS-INSU, IFREMER, and GENAVIR are gratefully acknowledged for their financial and technical support. F.S. was supported by a fellowship funded by IFREMER and CNRS. The data presented in this paper have been collected as part of an industrial project and are proprietary. The authors are grateful to Eramet, Technip and

Areva for their support. The reviewers are gratefully acknowledged. JD thanks Yves Lagabrielle for useful discussions on the geodynamics of the North Fiji and Lau basins. The Geological Survey of Norway (NGU) supported this research. This is IPGP contribution XXX.

References

Baker, E. T., et al. (2005), Hydrothermal activity on near-arc sections of back-arc ridges: results from the Mariana Trough and Lau Basin, *Geochem. Geophys. Geosyst.*, 6, Q09001.

Bird, P. (2003), An updated digital model of plate boundaries, *Geochem. Geophys. Geosyst.*, *4 (3)*, 1027, https://doi:10.1029/2001GC000252.

Brocher, T. M., T., Brink, and S., Uri (1985), Variations in oceanic layer 2 elastic velocities and their correlation to lithospheric flexure, *AGU fall meeting*. Anonymous.

Caratori Tontini, F., B., Davy, C. E. J., de Ronde, R. W., Embley, M., Leybourne, and M. A., Tivey (2012), Crustal magnetization of Brothers Volcano, New Zealand, measured by autonomous underwater vehicles: Geophysical expression of a submarine hydrothermal system, *Econ. Geol.*, *107* 1571-1581, https://doi:10.2113/econgeo.107.8.1571.

Fouquet, Y., et al. (1991), Hydrothermal activity in the Lau back-arc basin: sulfides and water chemistry, *Geology*, *19 (4)*, 303-306.

Fouquet, Y., et al. (1993), Metallogenesis in back-arc environments – the Lau Basin example, *Econ. Geol.*, *88 (8)*, 2154-2181.

Fouquet et al., (2015), Discovery of Extensive Hydrothermal Fields in the Wallis and Futuna Back-Arc Environment (SW Pacific), Mineral resources in a sustainable world, 13th SGA Biennial Meeting, Proceedings, Volume 3.

Fouquet, Y., et al., (2018), Volcanic and hydrothermal processes in submarine calderas: the Kulo Lasi example (SW Pacific). *Ore Geol. Rev.*, *99*, 314-343, https://doi.org/10/1016/j.oreegorev.2018.06.006.

Fujii, M., et al. (2015), High-resolution magnetic signature of active hydrothermal systems in the back-arc spreading region of the southern Mariana Trough, *J. Geophys. Res Solid Earth*, *120*, 2821-2838, doi:10.1002/2014JB011714.

Grzesczyk, A., et al. (1987), Pétrographie et minéralogie des îles Futuna et Alofi, TOM de Wallis-et-Futuna (Pacifique Sud-Ouest), *Comptes Rendus de l'Académie des Sciences, Série 2, Mécanique, Physique, Chimie, Sciences de l'Univers, Sciences de la Terre*, *305 (2)*, 93-98.

Grzesczyk, A., et al. (1988), Geologie des iles Futuna et Alofi (T.O.M. des îles Wallis-et-Futuna, Pacifique Sud-Ouest) Données préliminaires, *Géologie de la France*, *1988 (2F3)*, 131-134.

Grzesczyk, A., et al. (1991a), Mise en évidence d'un volcanisme transitionnel Pliocène supérieur sur Futuna et Alofi (SW Pacifique) : un nouveau témoin de l'évolution géodynamique Nord-Tonga, *Comptes Rendus de l'Académie des Sciences, Série 2, Mécanique, Physique, Chimie, Sciences de l'Univers, Sciences de la Terre*, *312 (7)*, 713-720.

Grzesczyk A., et al. (1991b), The upper Pliocene transitional eruptive stage on Futuna and Alofi islands, SE Pacific, trace element and Sr-Nd isotopic evidence for a heterogeneous mantle contribution, *Terra Abstracts*, *03 (1)*, 425-426.

Guivel, C., Y., Lagabrielle, J. P., Eissen, L., Dosso, and E., Ruellan (1997), Mise en place de basaltes enrichis le long d'un axe d'accrétion actif en domaine d'arrière-arc (dorsale Sud Pandora-Tripartite, bassin Nord-Fijien, Sud-Ouest Pacifique), *Comptes Rendus de l'Académie des Sciences de Paris, Sciences de l'Univers, Sciences de la Terre*. *325*, 651-658.

Honsho, C., et al. (2009), Magnetic structure of a slow spreading ridge segment: Insight from near-bottom magnetic measurements onboard a submersible*, J. Geophys. Res.*, *114*, B05101, https://doi:10.1029/2008JB005915.

Honsho, C., T., Ura, and K. Tamaki (2012), The inversion of deep-sea magnetic anomalies using Akaike's Bayesian information criterion, *J. Geophys. Res., 117*, B01105, https://doi:10.1029/2011JB008611.

Honsho, C., T., Ura, and K. Kim (2013), Deep-sea magnetic vector anomalies over the Hakurei hydrothermal field and the Bayonnaise knoll caldera, Izu-Ogasawara arc, Japan, *J. Geophys. Res.*, *118*, 5147-5164, https://doi:10.1002/jgrb.50382.

Isezaki, N. (1986), A new shipboard three-component magnetometer, *Geophysics*, *51*, 1992-1998.

Jackson, M. G. et al (2010), Samoan hotspot track on a "hotspot highway": Implications for mantle plumes and a deep Samoan mantle source, *Geochem. Geophys. Geosyst*. *11 (12)*, Q12009, doi:10.1029/2010GC003232.

Jenner, F. E., et al. (2012), Chalcophile element systematics in volcanic glasses from the northwestern Lau Basin, *Geochem. Geophys. Geosyst*. *13 (6)*, Q06014, doi:10.1029/2012GC004088.

Konn, C., et al. (2016), Extensive hydrothermal activity revealed by multi-tracer survey in the Wallis and Futuna region (SW Pacific), *Deep Sea Res. Part 1: Oceanographic Res. Pap.*, *116*, 127-144.

Konn, C., et al. (2018), Organic Gas and Element geochemistry of hydrothermal fluids of the newly discovered extensive hydrothermal area in the Wallis and Futuna Region (SW Pacific), *Geofluids*, https://doi.org/10.1155/2018/7692839.

Labanieh, S., et al. (2011), Origin of the seamounts near Futuna Island, SW Pacific, *Goldschmidt Conference Abstracts*.

Lagabrielle, Y., et al. (1996), Active oceanic spreading in the northern North Fiji Basin. Results of the NOFI cruise of R/V L'Atalante, *Mar. Geophys.*, *18*, 225-247.

Lagabrielle, Y., J., Goslin H., Martin, J. L., Thirot, and J. M., Auzende (1997), Multiple active spreading centers in the hot North Fiji Basin (SW Pacific): a possible model for Archean ocean dynamics? *Earth Planet. Sci. Lett.*, *149*, 1-13.

Lupton, J., et al. (2012), Hydrothermal activity in the northwest Lau Backarc Basin: Evidence from water column measurements, *Geochem. Geophys. Geosyst.*, *13 (5)*, Q0AF04.

Lupton, J., et al. (2015), Helium isotope, C/^{3}He, and Ba-Nb-Ti signatures in the northern Lau Basin: distinguishing arc, back-arc and hotspot affinities, *Geochem. Geophys. Geosyst.*, *16 (4)*, 1133-1155.

Pelletier, B., S., Calmant, and R., Pillet (1998), Current tectonics of the Tonga-New Hebrides Region, *Earth Planet. Sci. Lett., 164 (1-2)*, 263-276.

Pelletier, B., et al. (2001), Newly identified segments of the Pacific-Australia plate boundary along the North Fiji transform zone, *Earth Planet. Sci. Lett., 193 (3F4)*, 347-358.

Price, A., et al. (2016), Geochemical evidence in the Northeast Lau Basin for subduction of the Cook-Austral volcanic chain in the Tonga Trench, *Geochem. Geophys. Geosyst.*, *17*, 1694-1724, https://doi:10.1002/2015GC006237.

Ruellan, E., and Y., Lagabrielle (2005), Subductions et ouvertures océaniques dans le Sud-Ouest Pacifique, *Géomorphologie relief processus environnement*, *2*, https://doi:10.4000/geomorphologie.307.

Sleeper, J. D., and F. Martinez (2016), Geology and kinematics of the Niuafo'ou microplate in the northern Lau Basin, *J. Geophys. Res. Solid Earth*, *121*, 4852-4875, doi:10.1002/2016JB013051.

Szitkar, F., J., Dyment, Y., Fouquet, and Y., Choi (2014), What causes low magnetization at basalt-hosted hydrothermal sites? Insights from inactive site Krasnov (MAR 16°38′N), *Geochem. Geophys. Geosyst.*, *15*, 1441-1451, doi:10.1002/2014GC005284.

Szitkar, F., J., Dyment, Y., Fouquet, Y., Choi, and C., Honsho (2015a), Absolute magnetization of the seafloor at a basalt-hosted hydrothermal site: Insights from a deep-sea submersible survey, *Geophys. Res. Lett.*, *42*, doi:10.1002/2014GL062791.

Szitkar, F., S., Petersen, F., Caratori Tontini, and L., Cocchi, (2015b), High-resolution magnetics reveal the deep structure of a volcanic arc-related basalt-hosted hydrothermal site (Palinuro, Tyrrhenian Sea), *Geochem. Geophys. Geosyst.*, *16*, http://dx.doi.org/10.1002/2015GC005769.

Szitkar, F., et al. (2017), Magnetic exploration of a low-temperature ultramafic-hosted hydrothermal site (Lost City, 30°N, MAR), *Earth Planet. Sci. Lett.*, *461*, 40-45, http://dx.doi.org/10.1016/j.epsl.2016.12.033.

Tivey, M. A., P. A., Rona, and H., Schouten (1993), Reduced crustal magnetization beneath the active sulfide mound, TAG hydrothermal field, Mid-Atlantic Ridge, at 26°N, *Earth Planet. Sci. Lett.*, *115*, 101-115, https://doi:10.1016/0012-821X (93)90216-V.

Wright, D. J., S. H., Bloomer, C. J., MacLeod, B., Taylor, and A. M., Goodliffe (2000), Bathymetry of the Tonga Trench and Forearc: A Map Series, *Marine Geophys. Res.*, *21 (5)*, 489-512, https://doi: 10.1023/A:1026514914220.

Zellmer, K. E., and B., Taylor (2001), A three-plate kinematic model for Lau Basin opening, *Geochem. Geophys. Geosystems, 2(5),* https://doi:10.1029/2000GC000106.

Figure captions

Figure 1: (A) Regional bathymetry and tectonic structures of the North Fiji and Lau basins. Bathymetric background from Ruellan and Lagabrielle (2005). HHR, Hazel-Holmes Ridge; SPR, South Pandora Ridge; TrR, Tripartite Ridge; NCR, North Cikopia Ridge, FR, Futuna Ridge; NWL, Northwest Lau Ridge; NEL, Northeast Lau Ridge, NfR, Niuafo'ou Ridge; MTJ, Mangatolu

Triple Junction; NFTF, North Fiji Transform Fault; PR, Peggy Ridge Transform Fault, CLR, Central Lau Spreading Center; VFR, Valu Fa Spreading Center. Many large volcanic ridges and edifices lie in a 200 km-wide stripe south of the fossil Vitiaz subduction zone. (B) Close-up on the Futuna area based on the bathymetric data from cruises ALAUFI and FUTUNA 1, 2 and 3, with Futuna and Alofi Islands in the center of the map. The bathymetry to the Southeast of the islands is generally shallower than to the West, marking the SEFVZ. The Kulo Lasi Caldera, Fatu Kapa and Tasi Tulo areas are located within the dashed rectangle whereas the inactive Ono Caldera is located slightly further to the Southwest.

Figure 2: (A) High-resolution bathymetry of the Kulo Lasi Caldera. The smooth bathymetry at its bottom corresponds to new and mostly basaltic lava flows with some andesitic flows. (B) Equivalent magnetization derived from the AUV magnetic anomalies using Honsho's Bayesian inversion (2012). (C) Reduced-to-the-Pole magnetic anomaly computed from the equivalent magnetization. The bottom of the caldera is associated with a relatively weak magnetic anomaly by comparison with the top of the two flanking volcanoes. To the Northeast, an elongated negative magnetic anomaly corresponds to a hydrothermally active area, in accordance with previous studies in basaltic (e.g., Tivey et al, 1993) and andesitic (Fujii et al, 2015) contexts.

Figure 3: (A) High-resolution bathymetry of the inactive Ono Caldera. Its bottom is smoothened by sediment coverage. (B) Equivalent magnetization derived from the AUV magnetic anomalies as in Fig. 2B. (C) Reduced-to-the-Pole magnetic anomaly as in Fig. 2C. The RTP anomaly is opposed to that of the Kulo Lasi Caldera (Fig. 2C) and requires a reversed

magnetic polarity. (D) Magnetization intensity and polarity along the DSS *Nautile* path. The polarity is consistently reversed, confirming the result from the AUV data.

Figure 4: (A) High-resolution bathymetry of the Fatu Kapa area. The central graben bisecting the area hosts the studied volcanoes in its eastern and western parts. (B) Equivalent magnetization derived from the AUV magnetic anomalies as in Fig. 2B for the studied volcanoes. (C) Reduced-to-the-Pole magnetic anomaly as Fig. 2C for the studied volcanoes. The volcanoes are associated with a positive equivalent magnetization and RTP magnetic anomalies consistent with a normal magnetic polarity.

Figure 5: (A) High-resolution bathymetry of the Tasi Tulo area. (B) Equivalent magnetization derived from the AUV magnetic anomalies as in Fig. 2B. (C) Reduced-to-the-Pole magnetic anomaly as Fig. 2C. Two volcanic ridges show a positive equivalent magnetization and RTP anomaly, whereas a series of at least six flat large volcanoes show variable magnetic signatures consistent with either normal or reverse magnetic polarities. B and E have a magnetic signature comparable to that of the Kulo Lasi whereas D and F are similar to Ono, with a rim of negative RTP magnetic anomaly encompassing an area of weaker magnetic signature.

Figure 6: (A) See Fig. 1A. (B) Regional bathymetry and tectonic structures in the northern Lau Basin. Abbreviations: see Fig. 1A and KL, Kulo Lasi; On, Ono; FK, Fatu Kapa; and TT, Tasi Tulo. (C) Plates and their inferred relative motions in the northern Lau Basin (modified after Zellmer and Taylor, 2001 and Bird, 2003). Plain colors describe individual plates: AUS, Australian Plate; PAC, Pacific Plate; TON, Tonga Plate, NIU, Niuafo'ou Plate, FUT, Futuna

Plate; AOP: An Other Plate; YAO: Yet Another One. The three later plates are proposed in this study. Double-headed arrows: diverging motion, Double arrows: transform motion; Single-headed arrows: converging motion.

Declaration of interests

☒ The authors declare that they have no known competing financial interests or personal relationships that could have appeared to influence the work reported in this paper.

☐The authors declare the following financial interests/personal relationships which may be considered as potential competing interests:

Highlights

The seafloor southeast of Futuna Island (Southwestern Pacific Ocean) is associated with intense volcanic and tectonic activity.

High-resolution magnetic data reveal the existence of calderas older and younger than the last geomagnetic polarity reversal.

Continuous and sparse volcanic activity has occurred for the last few million years.

Volcanic activity is driven by the melting of the underlying mantle with a contribution of the nearby Samoa hotspot.

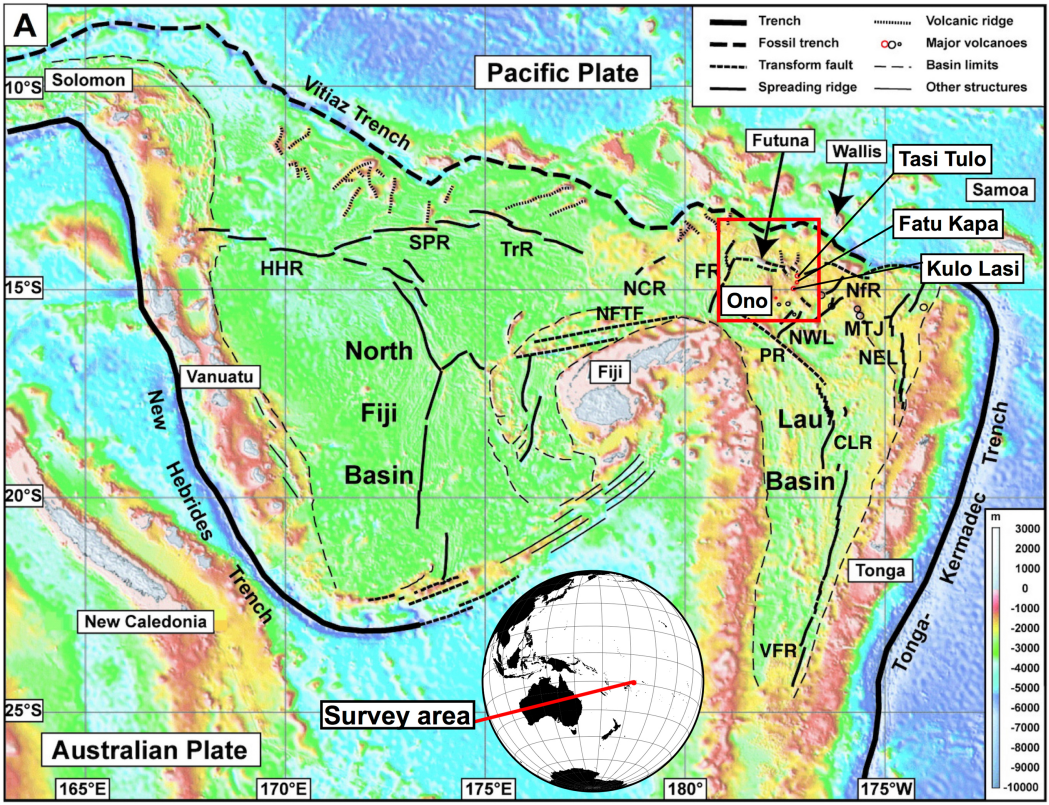
A
Trench
Fossil trench
Transform fault
Spreading ridge
Volcanic ridge
Major volcanoes
Basin limits
Other structures
Pacific Plate
Solomon
Vitiaz Trench
Futuna
Wallis
Tasi Tulo
Samoa
Fatu Kapa
Kulo Lasi
SPR
TrR
HHR
FR
NCR
NFTF
Ono
NfR
MTJ
NWL
PR
NEL
North
Fiji
Basin
Fiji
Vanuatu
New Hebrides Trench
Lau
CLR
Basin
Tonga
Tonga-Kermadec Trench
VFR
New Caledonia
Survey area
Australian Plate
10°S
15°S
20°S
25°S
165°E
170°E
175°E
180°
175°W
m
3000
2000
1000
0
-1000
-2000
-3000
-4000
-5000
-6000
-7000
-8000
-9000
-10000

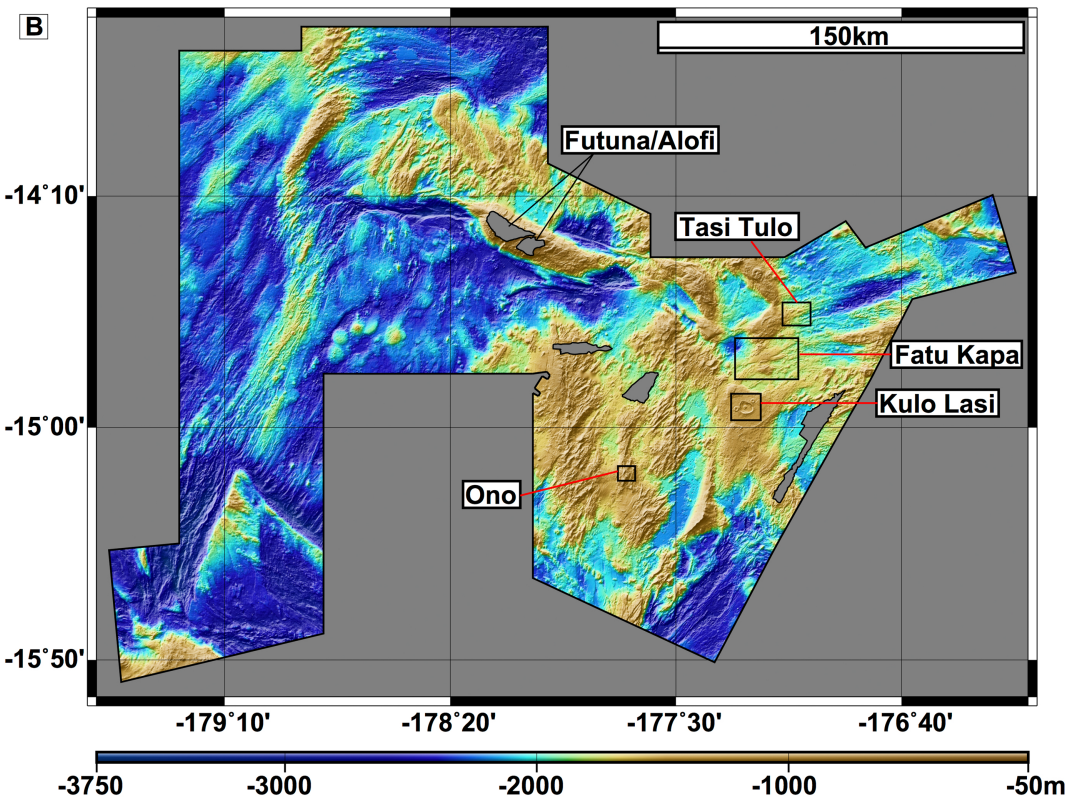
B
150km
Futuna/Alofi
Tasi Tulo
Fatu Kapa
Kulo Lasi
Ono
-14°10'
-15°00'
-15°50'
-179°10'
-178°20'
-177°30'
-176°40'
-3750
-3000
-2000
-1000
-50m

Figure 1

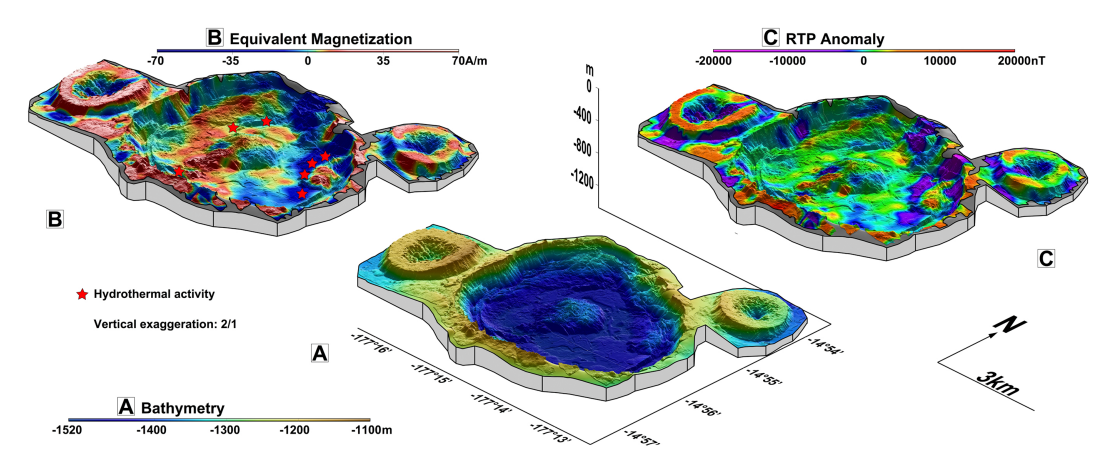
B Equivalent Magnetization
-70
-35
0
35
70A/m
B
C RTP Anomaly
-20000
-10000
0
10000
20000nT
m
0
-400
-800
-1200
C
Hydrothermal activity
Vertical exaggeration: 2/1
A
-117°16'
-117°15'
-117°14'
-117°13'
-14°54'
-14°55'
-14°56'
-14°57'
N
3km
A Bathymetry
-1520
-1400
-1300
-1200
-1100m

Figure 2

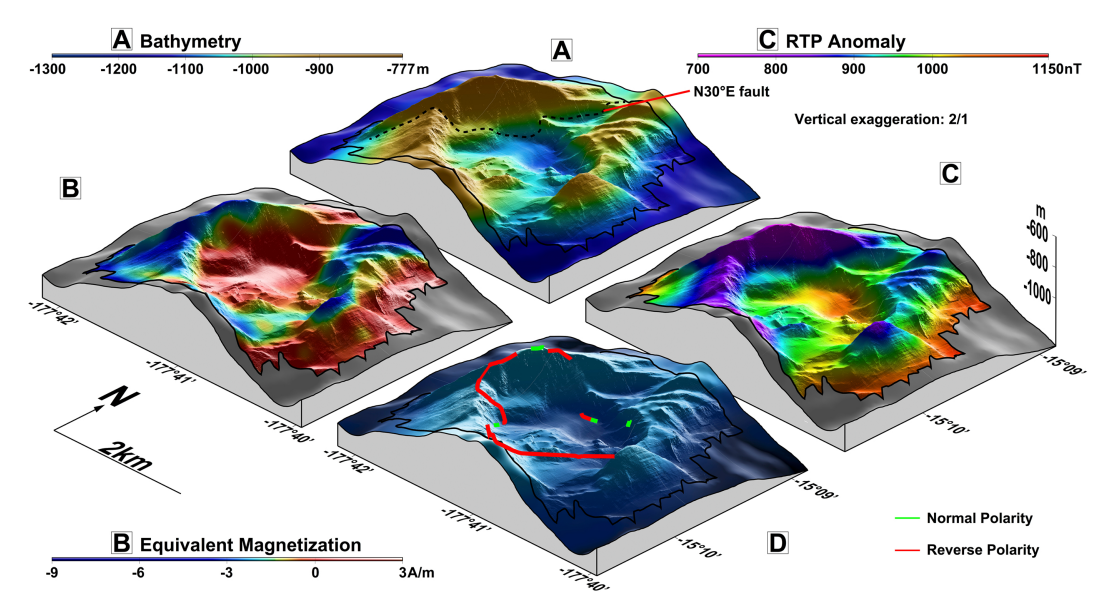
A Bathymetry
-1300 -1200 -1100 -1000 -900 -777m
A
C RTP Anomaly
700 800 900 1000 1150nT
N30°E fault
Vertical exaggeration: 2/1
B
C
m
-600
-800
-1000
-177°42'
-177°41'
-177°40'
-15°09'
-15°10'
N
2Km
D
B Equivalent Magnetization
-9 -6 -3 0 3A/m
Normal Polarity
Reverse Polarity

Figure 3

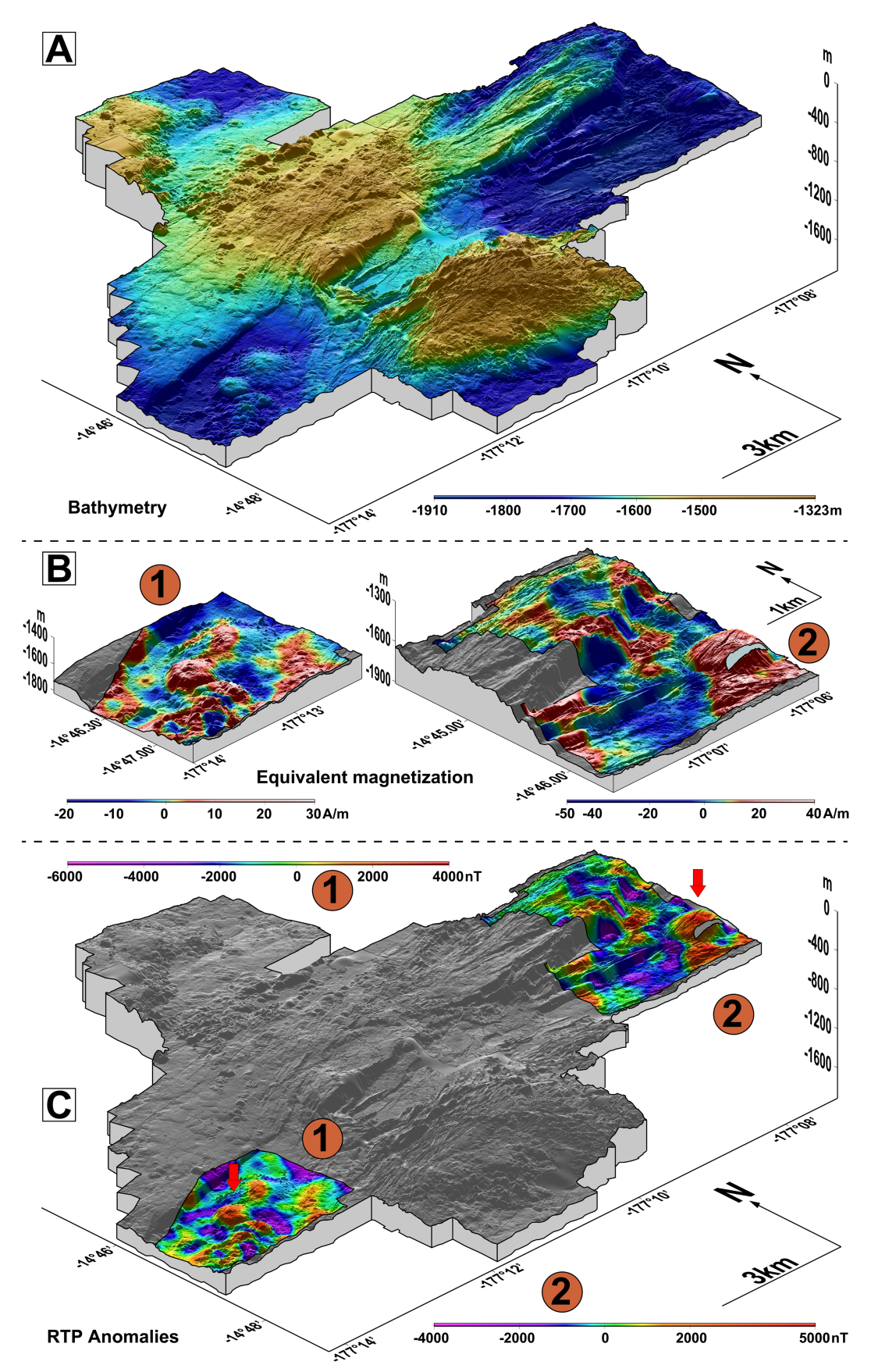
A
m
0
-400
-800
-1200
-1600
-14° 46'
-14° 48'
-177° 14'
-177° 12'
-177° 10'
-177° 08'
N
3km
Bathymetry
-1910
-1800
-1700
-1600
-1500
-1323m
B
1
m
-1400
-1600
-1800
-14° 46.30'
-14° 47.00'
-177° 14'
-177° 13'
m
-1300
-1600
-1900
-14° 45.00'
-14° 46.00'
-177° 07'
-177° 06'
N
1km
2
Equivalent magnetization
-20
-10
0
10
20
30 A/m
-50
-40
-20
0
20
40 A/m
-6000
-4000
-2000
0
2000
4000 nT
1
2
C
1
2
RTP Anomalies
-4000
-2000
0
2000
5000 nT

Figure 4

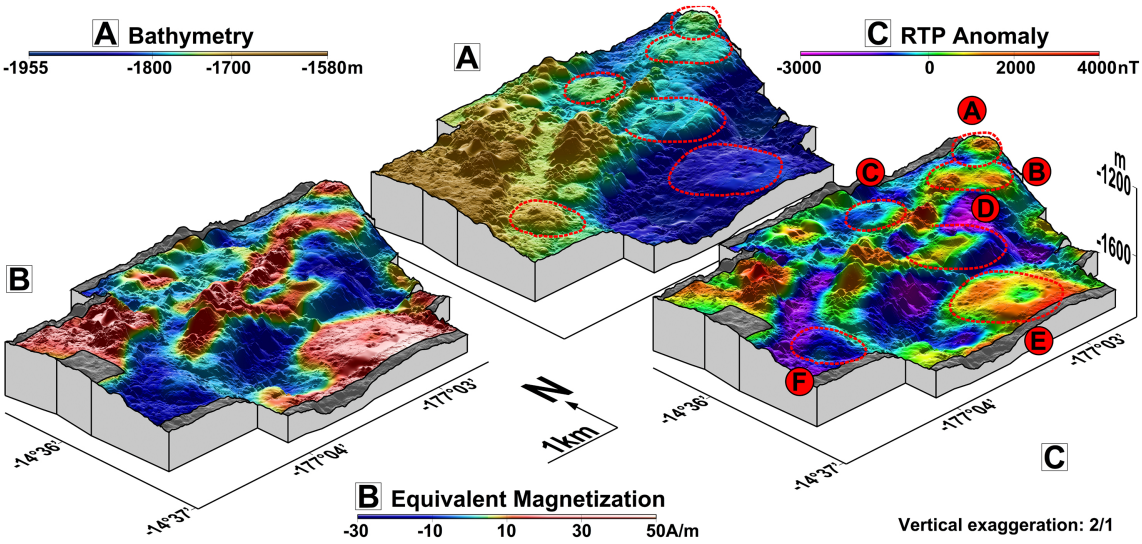
A Bathymetry
-1955
-1800
-1700
-1580m
A
C RTP Anomaly
-3000
0
2000
4000nT
A
B
C
D
E
F
m
-1200
-1600
B
-14°36'
-14°37'
-177°04'
-177°03'
N
1km
B Equivalent Magnetization
-30
-10
10
30
50A/m
C
Vertical exaggeration: 2/1

Figure 5

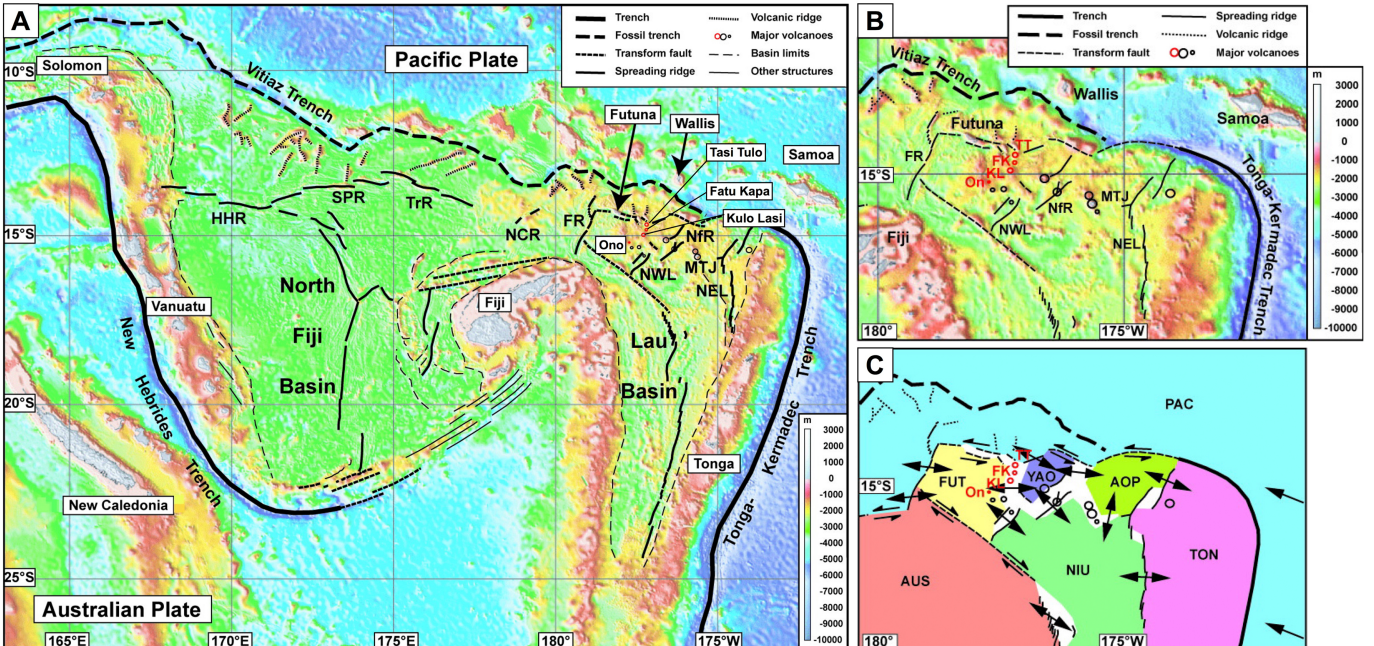
A
Trench
Fossil trench
Transform fault
Spreading ridge
Volcanic ridge
Major volcanoes
Basin limits
Other structures
Pacific Plate
Solomon
Vitiaz Trench
Futuna
Wallis
Tasi Tulo
Samoa
Fatu Kapa
Kulo Lasi
SPR
TrR
HHR
NCR
FR
Ono
NfR
NWL
MTJ
NEL
North Fiji Basin
Fiji
Lau Basin
Vanuatu
New Hebrides Trench
Tonga
Tonga-Kermadec Trench
New Caledonia
Australian Plate
10°S
15°S
20°S
25°S
165°E
170°E
175°E
180°
175°W
m
3000
2000
1000
0
-1000
-2000
-3000
-4000
-5000
-6000
-7000
-8000
-9000
-10000
B
Trench
Fossil trench
Transform fault
Spreading ridge
Volcanic ridge
Major volcanoes
Vitiaz Trench
Wallis
Futuna
Samoa
FR
FK
KL
On
T
NfR
MTJ
NWL
NEL
Fiji
Tonga-Kermadec Trench
15°S
180°
175°W
m
3000
2000
1000
0
-1000
-2000
-3000
-4000
-5000
-6000
-7000
-8000
-9000
-10000
C
PAC
FUT
YAO
AOP
TON
NIU
AUS
FK
KL
On
T
15°S
180°
175°W

Figure 6